

Finger Trajectory Generation for Planar Dexterous Micro-Manipulation

Jean-Antoine Seon, Redwan Dahmouche, Benoit Brazey, Michaël Gauthier

Abstract—Dexterous micro-manipulation is a promising way to perform complex manipulation in micro-scale. Current dexterous micro-handling solutions are often limited to small amplitude rotations (around 90°) and to simple shaped objects (such as squares). Our approach consists in developing in-hand micro-manipulation techniques using dexterous micro-hands, taking advantage of adhesion forces, to manipulate arbitrary shaped objects. This paper focuses on the trajectory generation of a dexterous micro-hand to achieve automated repositioning. The statistical results on the generated trajectories show that the adhesion forces in micro-scale can be exploited to enhance micro-manipulation.

I. INTRODUCTION

Dexterous manipulation has been an active field of research in macro-scale [1] [2] [3] but has not been largely investigated in micro-scale. Indeed, micro-manipulations are usually limited to simple pick and place operations [4] [5] [6] even if off-the-shelf dexterous manipulator are available [7].

In facts, micro-object's rotation control is one of the most critical steps in micro-manipulation. Rotation are usually obtained in two ways. The first one, which is the most common industrial architecture in macro-scale, consists in using a basic tweezer placed on a robot which rotates the carried gripper. The second way consists in using dexterous micro-hand to perform in-hand rotations [8] [9] [10]. The first approach does not enable to reach sufficient accuracy in micro-scale, especially when several rotations are required. Indeed, backlash and eccentricity are usually larger than $10\mu\text{m}$ [11]. The second one seems to be promising but requires a dexterous gripper and advanced trajectory generator.

Moreover, in micro-scale, gravitational and inertial forces are overpowered by the surface forces such as Van der Waals, electrostatic and capillary forces [12]. These sticky forces change the manipulation paradigm as the objects stick to both the manipulator and the substrate [13]. Thus planning trajectory for dexterous manipulation in micro-scale is significantly different from macro-scale.

Contrary to various approaches that try to minimize the adhesion effect in order to fallback to macro-scale manipulation [14] [15], we propose in this paper to exploit these adhesion forces that can contribute to the stability of the object during the manipulation.

The main contribution of this paper is the development of a trajectory planner for in-hand dexterous micro-manipulation that takes advantage of adhesion forces. Original fingers

trajectories are proposed and the added value of the adhesive forces on the micro-manipulation is demonstrated.

The next section gives an overview of the related work in automatic dexterous micro-manipulation while Section III gives a general formalization of this problem. Section IV details our methodology to compute stable grasps and generate trajectories. Then, section V presents some trajectories for three fingers manipulation with and without sticky fingers in the case of planar objects.

II. RELATED WORK

One of the first work in the dexterous micro-manipulation field can be assigned to Thompson and Fearing with the ortho-tweezers [16]. In this system, two orthogonal fingers have been used to manipulate micro-blocks ($200\mu\text{m}\times 200\mu\text{m}\times 100\mu\text{m}$). The manipulation process is performed using manipulation primitives such as grasp the object, rotate along z-axis, etc. Since a two fingers hand has limited dexterity, a static external block is used to achieved a two axis rotation.

In 2006, Zhou *et al.* has developed a 6 degrees of freedom manipulator able to perform automatic in-hand manipulation [8]. The manipulator uses only two fingers to manipulate micro-blocks ($300\mu\text{m}\times 300\mu\text{m}\times 100\mu\text{m}$). In both methods, fingers' rolling on the object during the rotation is neglected and no finger gaiting is used which limits the rotation amplitude.

Recently, Brazey *et al.* have developed a dexterous micro-manipulation system able to perform large rotations of micro-objects [10]. The setup is composed of three fingers each one having two degrees of freedom. Figure 1 shows a 180° rotation of a $200\mu\text{m}$ micro-square (see attached multimedia file). The manipulation process is fully automatic and is based on trajectories generated using manipulation primitives.

Contrarily to the dexterous manipulation approaches presented in this section, the proposed method is not limited to squared objects since arbitrary shapes are considered. In addition, the rolling constraint of the fingers during the object rotation is explicitly taken into account and the sticky forces that may exist in the micro-scale are exploited by the proposed approach.

III. MODELING AND BACKGROUND

In this section, we are going to show how the formalization of manipulation is impacted by adhesion forces.

A. Grasping Forces

Let us consider the general case of six DOF manipulation using N fingers. In order to manipulate the object, fingers

The authors are with FEMTO-ST Institute, AS2M department, Université Bourgogne Franche-Comté, Université de Franche-Comté/CNRS/ENSMM/UTBM, 24 rue Savary, 25000 Besançon, France. ja.seon@femto-st.fr

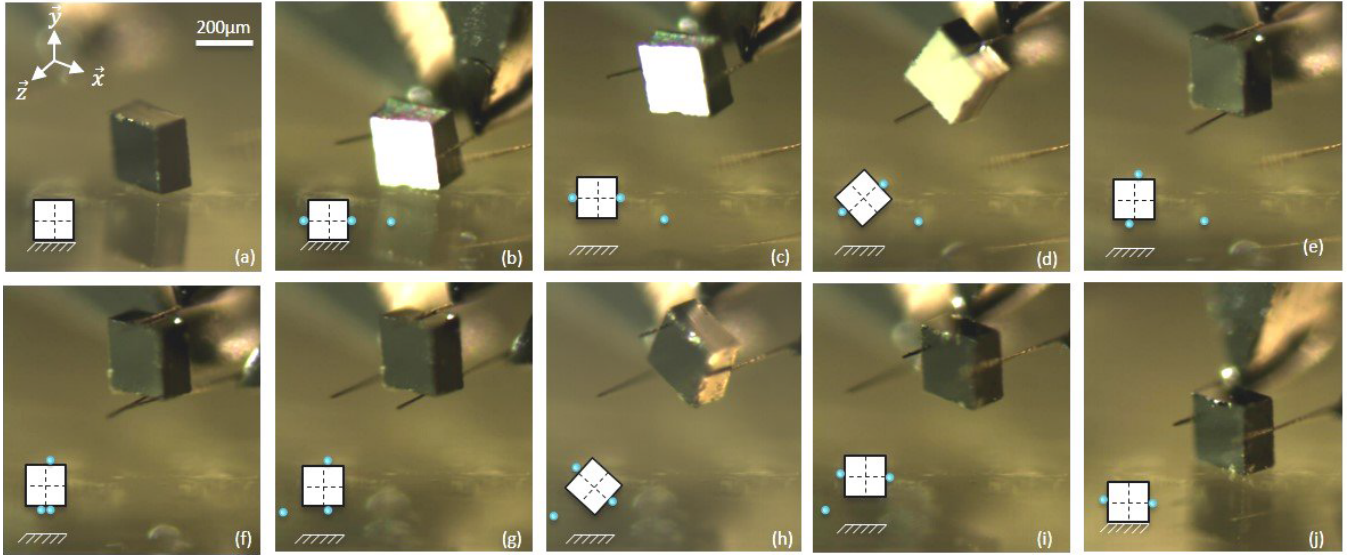


Fig. 1: Illustration of an automatic 180° rotation performed using 3 fingers on our manipulation setup [10].

must apply a grasping force on the object surface. The most common modeling of the applied forces in macro-scale is the *Coulomb law*. This means that, there is no slippage as far as the exerted force lies in a three dimensions cone:

$$\sqrt{f_{t1}^2 + f_{t2}^2} \leq \mu f_n \quad (1)$$

where f_{t1} and f_{t2} are tangential component of the force, f_n is the normal component and μ is the friction coefficient.

In the case of micro-manipulation, this contact law is slightly modified. Indeed, adhesion acts as an attractive force (f_{po}) between the finger and the manipulated object. This force, called pull-off force, represents the force required to detach the finger from the object. In presence of this force, the Coulomb law can be rewritten as follows:

$$\sqrt{f_{t1}^2 + f_{t2}^2} \leq \mu(f_n + f_{po}) \quad (2)$$

The effect of this attractive force on the slippage limit condition is that the friction cone is shifted as depicted in Fig.2. In addition, contrary to the macro-scale, where only positive grasping forces can be applied (push the object), in micro-scale, it is possible to apply negatives grasping forces (pull the object) as long as the force lies in the modified friction cone.

B. Equilibrium

When N fingers grasp an object, the grasping forces must be well balanced in order to reach the static equilibrium. Thus, the following equation must be satisfied:

$$-w_{ext} = G \cdot f_c = \sum_{i=1}^N w_{c_i} \quad (3)$$

where w_{ext} is the external wrench (force and moment) applied on the object, the matrix $G \in \mathfrak{R}^{6 \times 3N}$ is called the grasp matrix [17] which depends on the contact position, $f_c \in \mathfrak{R}^{3N}$ is the

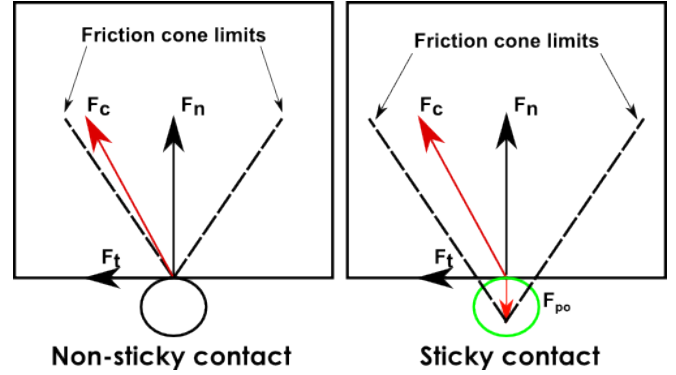


Fig. 2: Side view of the impact of pull-off force on the friction cone.

vector containing the N grasping forces and $w_{c_i} \in \mathfrak{R}^6$ is the i^{th} grasping wrench.

Given a set of contact points, the equilibrium problem consists in finding a set of grasping forces f_c which respects equation (3) and the non-slippage constraint defined by (2). This problem can be rewritten using the limits of the friction cones. Indeed, the grasping wrench applied at the i^{th} contact point is a linear combination of wrenches that approximate the cone:

$$\begin{cases} w_{c_i} = \sum_j \alpha_{i,j} \cdot w_{l_{i,j}} + \beta_i \cdot w_{p_{o_i}} \\ \alpha_{i,j} \geq 0 \\ 1 \geq \beta_i \geq 0 \end{cases} \quad (4)$$

where $w_{l_{i,j}}$ is one wrench that approximate the i^{th} friction cone, $w_{p_{o_i}}$ is the wrench induced by pull-off forces (sticking effect), and $\alpha_{i,j}$ and β_i are coefficients that must be positive to stay inside the friction cone. Note that in macro-manipulation, $w_{p_{o_i}} = 0$. Then, the equilibrium problem of an N fingers grasp can be rewritten as a function of the N friction cones wrenches:

$$-w_{ext} = \sum_{i=1}^N w_{c_i} = \sum_{i=1}^N \left(\sum_j \alpha_{i,j} \cdot w_{l_{i,j}} + \beta_i \cdot w_{p_{o_i}} \right). \quad (5)$$

Thus, the equilibrium problem is equivalent to find a set of positive $(\alpha_{i,j}, \beta_i)$ (not all of them null) verifying the previous equation. Since inertial forces of micro-objects are negligible, the condition to perform stable micro-manipulation is that the equilibrium condition defined by (5) is verified along the manipulation trajectory.

C. Pull-off Forces and Reconfigurations

In addition, the pull-off force between the fingers and the object, that contribute to stabilize the object during the grasping, becomes a perturbation force during finger gaiting (detaching a finger from the object and eventually repositioning it). During this critical step, the remaining grasping fingers must compensate for the pull-off force caused by the removed finger to guarantee the object's stability:

$$-w_{ext} - w_{p_o} = G \cdot f_c = \sum_{i=1}^{N-1} w_{c_i}, \quad (6)$$

where w_{p_o} is the wrench induced by the release of the N^{th} contact.

Considering (6), the reconfiguration problem consists in finding positive $(\alpha_{i,j}, \beta_i)$ (not all of them null) verifying the following equation:

$$-w_{ext} - w_{p_o} = \sum_{i=1}^{N-1} w_{c_i} = \sum_{i=1}^{N-1} \left(\sum_j \alpha_{i,j} \cdot w_{l_{i,j}} + \beta_i \cdot w_{p_{o_i}} \right). \quad (7)$$

In a formal way, the next section introduces a trajectory planer for dexterous manipulation which fulfill the constraints (5) and (7)

IV. DEXTEROUS MANIPULATION WITH ADHESION FORCES

Given an object shape and the number of fingers of the manipulation system, the first step of the trajectory generation consists in computing the set of stable grasps and the admissible finger gaiting configurations. This step can be achieved off-line and is done only once for a given object. The second step consists in navigating between these configurations to define a path from the initial configuration to the desired one.

A. Equilibrium and Reconfiguration Maps

The maps representing the set of equilibrium grasps during the different steps of the manipulation process are obtained by testing if the convex hull formed by the friction cones wrenches $(w_{l_{i,j}})$ contains the origin of the wrench space [18]. The existence of a solution, when external perturbations are considered, consists in testing if the convex hull contains the external wrench. Thus, equilibrium maps can be formalized as:

$$M_k = \left\{ (c_1, \dots, c_k) \in \mathfrak{R}^{(3 \times k)} \mid \begin{aligned} & -w_{ext} \in \text{Conv hull}(w_{l_{1,1}}, \dots, w_{l_{k,j}}) \end{aligned} \right\}, \quad (8)$$

where k is the number of contacts, c_k is a vector containing the contact coordinates on the object surface and $\text{Conv hull}(w_{l_{1,1}}, \dots, w_{l_{k,j}})$ represents the convex hull.

Figure 3 gives a representation of one of the M_k sets in the case of a cylindrical object without external forces. We chose to use the curvilinear abscissa as a coordinate of the contact point on the object. The colored areas on the left figure represent the equilibrium configurations for a two fingers grasp, without any pull-off forces. Since permuting the two contact points amounts to the same grasp, the equilibrium map shows a symmetry axis.

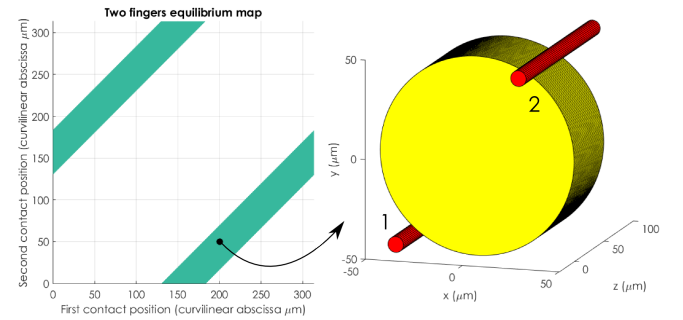


Fig. 3: Representation of the set M_2 for a 2D object, without considering adhesion (non-sticky behavior).

In finger gaiting, to guarantee that a given finger can be pulled-off from the object without disturbing the grasp, we ensure that the resulting wrench w_{p_o} , induced by the pull-off force f_{p_o} , is included in the convex hull formed by the friction cones' wrenches of the $N - 1$ remaining contacts. The reconfiguration maps can be formalized as follows:

$$D_k = \left\{ (c_1, \dots, c_k) \in \mathfrak{R}^{(3 \times k)} \mid \begin{aligned} & (c_1, \dots, c_{k-1}) \in M_{k-1}, \\ & -w_{p_{o,k}} \in \text{Conv hull}(w_{l_{1,1}}, \dots, w_{l_{k-1,j}}) \end{aligned} \right\}. \quad (9)$$

For each M_k ($k > 1$), it is possible to define a corresponding D_k .

Figure 4 (left) shows all the reconfiguration positions for a fixed third contact location in the case of a three fingers grasp (fingers are sticky). For instance, in the configuration represented in Fig.4 (right), removing finger 3 would disturb the grasp's equilibrium.

B. Planning Object Rotation

1) *Representation*: All the M_k maps can be seen as graph where every equilibrium position is a node. The goal is to navigate inside and between the maps to reach the desired object pose. In fact, navigating through a M_k map describes a direct manipulation of the object whereas navigating between two maps (M_i and M_j) characterizes finger gaiting. In this case, the reconfiguration maps D_k are also part of the graph.

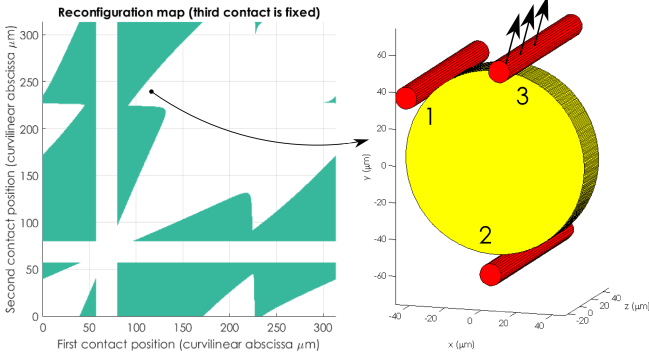


Fig. 4: Representation of the set D_3 for a fixed third contact location, considering adhesion (sticky behavior).

Each node in D_k is specifically used to link two adjacent sets (M_k and M_{k-1}) when a finger is removed. Moreover, as adhesion does not perturb the grasp when adding a finger, the link between M_k and M_{k+1} is direct.

2) *Navigation Constraints*: Two constraints must be taken into account when navigating in the maps. The first one is the rolling constraint. Indeed, in order to manipulate an object with N fingers considering rolling without sliding, all the fingers must roll the same distance and in the same direction on the object surface. Consequently, the rolling constraint induces a unique available path in a M_k map (depending on the radius of the fingers). Thus, each node in M_k has only two neighbors in the same map.

The second constraint is related to the collision between fingers. Collision tests are performed in order to guarantee that the generated trajectory is reachable by the manipulation setup.

3) *Trajectory Generation*: Trajectory generation consists in navigating in maps and one way to search through a graph is the A^* algorithm. This heuristic graph search algorithm provides a complete and optimal path between the initial and the goal node. A^* has been used in micro-manipulation [19] and also in micro-assembly [20] but based on our knowledge it has never been used for planning in-hand manipulations. We chose to implement an A^* algorithm for our trajectory planner in order to obtain optimal solutions.

4) *Algorithm Characteristics*: An important parameter of the graph search is the cost function used to characterise the distance between two nodes. Considering the way we can navigate through the graph, we define three cost functions corresponding to the three possible actions (rolling, putting a finger on the object, removing a finger from it).

For the first case (rolling), the cost function is defined as the rolling distance needed to go from the current node to the next one. This distance is the arc length between two positions on the object surface and is noted $L_{roll}(Node(i), Node(f))$.

As the fingers might be compliant, the fingers base displacement achieved by the actuator to detach the object from the object depends of the finger stiffness, its length and its radius. The cost, C_r , for detaching a finger from the object

corresponds to the minimal distance applied by the actuator to guarantee that the concerned finger is detached from the object.

For the last action (adding a finger), the cost function can take two values: (i) if the finger has not been used previously, then the cost function will be a non zero constant C_a . This value represents an approximation of the distance needed to put in contact the finger with the object (starting from the initial position). (ii) if the finger has been used previously, then the cost function will be an approximation of the distance between the last contact position and the new one. This distance is computed using the rolling distance between the two positions ($L_{rec}(Node(prev), Node(new))$) plus a non zero constant C_{ar} (with $C_a \gg C_{ar}$).

Moreover, the A^* algorithm requires defining an admissible heuristic. As the in-hand manipulation is a rotation, it is possible to define the heuristic as the remaining rotation from the current node to the desired one. Moreover, as rolling is used to rotate the object, it is also possible to define the heuristic as a distance. Indeed, consider that the finger used for the manipulation has a radius r_d and that rot is the rotation amplitude in radians. Then, at the initial node, the heuristic will be $d_{rot} = r_d \times rot$. Obviously this heuristic never overestimates the distance to the goal so it is an admissible heuristic for the considered cost functions.

V. RESULTS

The methodology presented in the previous section has been implemented and tested to generate trajectories for planar objects. In fact, in micro-assembly, most of the objects made using micro-fabrication techniques are planar objects so the results presented in this section are applicable micro-manipulation.

A. Sticky Fingers

In this simulation we consider manipulation with three fingers at most. This means that the nodes are represented by three maps: M_1 , M_2 , M_3 for manipulation and two: D_2 and D_3 for finger gaiting. In this study case, we consider the following cost functions: $L_{roll} = 0.6\mu\text{m}$, $C_a = 150\mu\text{m}$, $C_{ar} = 8\mu\text{m}$ and $C_r = 10\mu\text{m}$

Figure 5 illustrates the computed trajectory for a 140° rotation using fingers with a radius of $4\mu\text{m}$. The pull-off force between the object and the substrate is considered equal to $5\mu\text{N}$, the pull-off force between fingers and the object is equal to $1\mu\text{N}$ and the friction coefficient is constant on the surface (0.3). Moreover, the weight of the object is neglected which means that the external wrench is null.

Figure 5a represents the initial grasping configuration which is used to pick-up the object while Fig.5b to Fig.5e show the rotation. This manipulation is achieved without any finger reconfiguration (see multimedia file enclosed). Note that this manipulation process is not stable without the stickiness effect (see Fig.5e).

Figure 6 depicts the fingers trajectories represented in the x-y frame attached to the workspace.

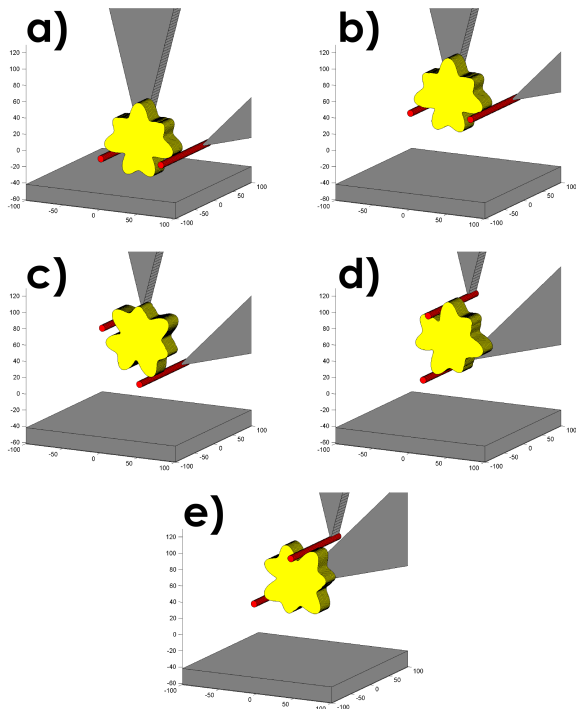


Fig. 5: Images sequence describing the trajectory generated by the planner for a 140° rotation with sticky fingers.

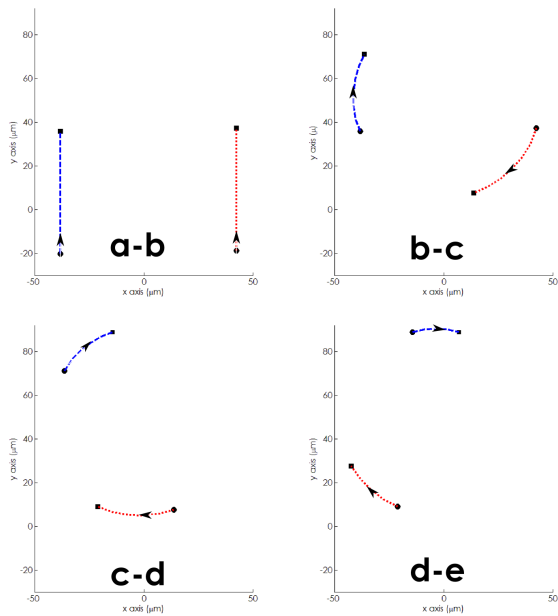


Fig. 6: Image sequence of the manipulation process. Each image represents the link between two grasps depicted in Fig.5

B. Non-sticky Fingers

In order to illustrate the impact of adhesion on the fingers' trajectory, we consider the same example but without the pull-off force (f_{po}) between fingers and the object.

Figure 7 illustrates the computed trajectory for a 140° rotation. It can be seen that the first grasp uses three fingers because two fingers grasps are not stable enough. Moreover, the manipulation process requires several finger reconfigurations: in Fig.7c left finger is reconfigured, in Fig.7e top and right fingers are reconfigured and finally in Fig.7g top and right fingers are reconfigured. Indeed, without stickiness effect, more reconfigurations are required to perform the same rotation (see attached multimedia file).

Figure 7b illustrates a particular behavior in which the calculated trajectory proceed to a counterclockwise rotation whereas the target orientation is clockwise. This is explained by the fact that the most optimal trajectory rolls away from the target to be able to perform finger gaiting before continuing the clockwise rotation. It shows that an optimal trajectory may includes both clockwise and counterclockwise rotations.

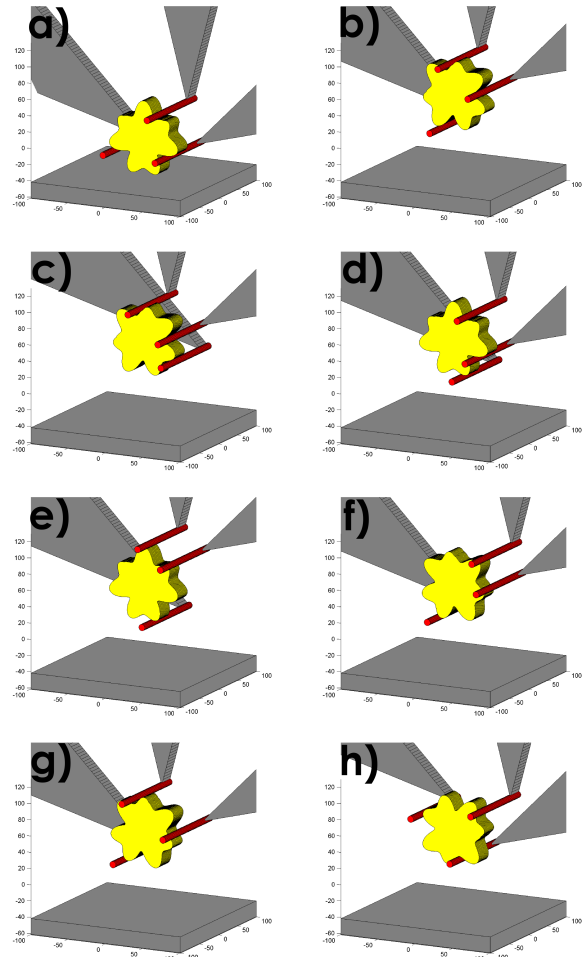


Fig. 7: Images sequence describing the trajectory generated by the planner for a 140° rotation with non-sticky fingers.

C. Impact of Adhesion Forces on Manipulation

The fact that adhesion forces have a great impact on dexterous manipulation is due to its stabilizing effect. Figures 8

shows this effect on the M_2 map of the arbitrary shaped object presented in Fig.5 and Fig.7. The blue and yellow areas correspond respectively to the M_2 maps with and without sticky fingers. As predicted, the area is significantly larger when pull-off forces are considered. This means that there is more options to manipulate the object in presence of adhesion (more stable nodes in the graph).

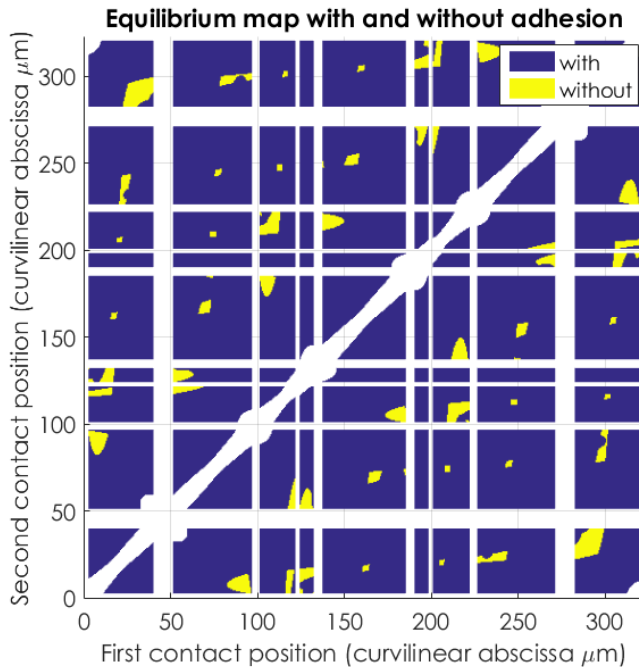


Fig. 8: Representation of the set M_2 (equilibrium map) with and without pull-off forces on the tested object.

Moreover, Fig.9 represents similar results for a reconfiguration map (D_3) for a fixed removed finger. It can be seen that, without adhesion, 100% of the equilibrium nodes in M_2 (Fig.8) are admissible reconfiguration nodes in D_3 (Fig.9). In contrast, with sticky fingers, the admissible reconfiguration nodes (D_3 in Fig.9) represent only around 18% of the equilibrium nodes (M_2 in Fig.8).

D. Sticky Fingers vs Non-Sticky Fingers

As shown previously, the manipulation process seems to require less finger gaiting steps and also less displacement of the fingers when adhesion forces are exploited. A statistical analysis has been done to confirm this property. Trajectories were generated with and without sticky fingers for the same object and with the same simulation parameters. In every test, the initial grasping configuration is chosen randomly.

Table 1 shows the statistical results considering 20 trajectories generating a 120° rotation. Considering that the fingers move at a constant velocity, the cost function which estimates the traveled distance can be converted into the manipulation time (note that the rolling distance is counted only once even if three fingers manipulate the object). It can be seen that the manipulation process cost less when using sticky fingers. Thus, the manipulation will be shorter with sticky

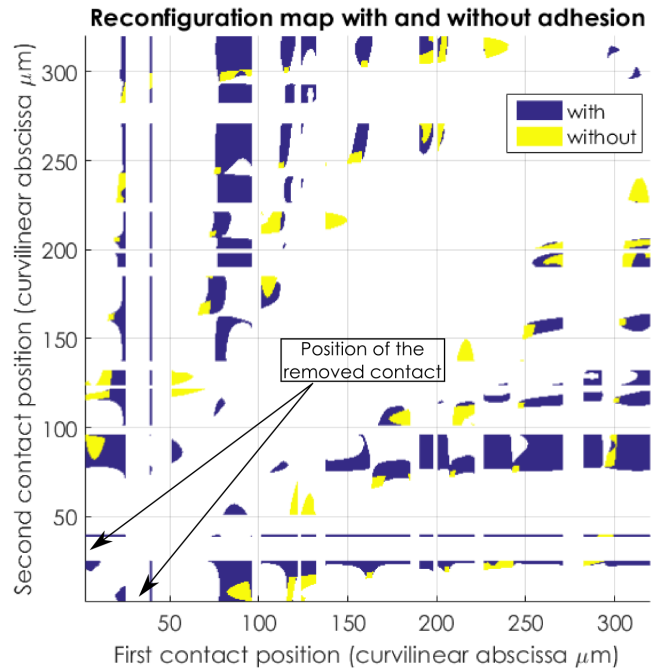


Fig. 9: Representation of the set D_3 with and without pull-off forces on the tested object.

fingers. Moreover, as shown by the standard deviation, the manipulation without sticky fingers is heavily dependent on the initial grasping configuration.

TABLE I: Statistical results for a 120° rotation. Cost is an estimation of the traveled distance during the manipulation process.

Finger type	Cost mean (μm)	Cost var (μm)	Explored node mean	Explored node var
Sticky	422	77.28	36	29
Non-Sticky	738	220	803	728

As a conclusion, this results shows that manipulations taking advantage of adhesion forces are more stable and require less finger reconfigurations and less displacements.

VI. CONCLUSION

In this paper, a trajectory planner for dexterous micro-manipulation taking into account adhesion forces has been presented. This planner is based on a A^* algorithm in order to generate optimal trajectories and takes into account the specificity of the micro-scale: the adhesion phenomena.

Our planner was validated in simulation considering different conditions of use (sticky and non-sticky fingers). The results show that in-hand micro-manipulation using adhesion forces is significantly different than macro-manipulation, and original trajectories have been generated. As adhesion phenomena cannot be neglected, we have shown that it can be a useful tool in the manipulation process (less dependent on the initial grasping configuration, an requiring less displacement).

The next step of this work is the validation these new trajectories on the experimental micro-manipulation setup developed in our laboratory. In addition, as the problem was formalized for three dimensions in-hand micro-manipulation, the current planner will be extended to non-planar objects. Moreover, fixing the adhesion parameter (in function of environmental parameters, chemical plating, ...) is also a promising way to improve dexterous micro-manipulation.

ACKNOWLEDGMENT

This work was supported by ACTION, the French ANR Labex no. "ANR-11-LABX-01-01" (<http://www.labex-action.fr>), by the Equipex ROBOTEX project (contract "ANR-10-EQPX-44-01") and by the Conseil Régional de Franche-Comté.

REFERENCES

- [1] Z. Li, J. Canny, and S. Sastry, "On motion planning for dexterous manipulation. i) the problem formulation," in *IEEE International Conference on Robotics and Automation*. IEEE, 1989, pp. 775–780.
- [2] A. M. Okamura, N. Smaby, and M. R. Cutkosky, "An overview of dexterous manipulation," in *IEEE International Conference on Robotics and Automation, 2000*, vol. 1. IEEE, 2000, pp. 255–262.
- [3] A. Bicchi and R. Sorrentino, "Dexterous manipulation through rolling," in *International Conference on Robotics and Automation*, vol. 1. IEEE, 1995, pp. 452–457.
- [4] H. Xie and S. Régnier, "Three-dimensional automated micromanipulation using a nanotip gripper with multi-feedback," *Journal of Micromechanics and Microengineering*, vol. 19, no. 7, p. 075009, 2009.
- [5] H. K. Chu, J. K. Mills, and W. L. Cleghorn, "Dual-arm micromanipulation and handling of objects through visual images," in *International Conference on Mechatronics and Automation (ICMA)*. IEEE, 2012, pp. 813–818.
- [6] J. T. Feddema, P. Xavier, and R. Brown, "Micro-assembly planning with van der waals force," *Journal of Micromechanics*, vol. 1, no. 2, pp. 139–153, 2001.
- [7] M. Gauthier, C. Clévy, D. Hériban, and P. Kallio, "Industrial tools for micromanipulation," in *Micro- and Nanomanipulation Tools*, Y. Sun and Xinyu, Eds., 2015, ch. 15, pp. 1–25.
- [8] Q. Zhou, P. Korhonen, J. Laitinen, and S. Sjövall, "Automatic dextrous microhandling based on a 6-dof microgripper," *Journal of Micromechanics*, vol. 3, no. 3, pp. 359–387, 2006.
- [9] K. Inoue, T. Tanikawa, and T. Arai, "Micro hand with two rotational fingers and manipulation of small objects by teleoperation," in *International Symposium on Micro-NanoMechatronics and Human Science*. IEEE, 2008, pp. 97–102.
- [10] B. Brazey, R. Dahmouche, J.-A. Seon, and M. Gauthier, "Experimental validation of in-hand planar orientation and translation at microscale," *Intelligent Service Robotics, Special Issue on Multi-scale Manipulation Toward Robotic Manufacturing Technologies*, 2015.
- [11] N. Tan, C. Clévy, G. J. Laurent, P. Sandoz, and N. Chaillet, "Characterization and compensation of xy micropositioning robots using vision and pseudo-periodic encoded patterns," in *IEEE International Conference on Robotics and Automation*. IEEE, 2014, pp. 2819–2824.
- [12] R. S. Fearing, "Survey of sticking effects for micro parts handling," in *IEEE/RSJ International Conference on Intelligent Robots and Systems*, vol. 2. IEEE, 1995, pp. 212–217.
- [13] N. Chaillet and S. Régnier, *Microrobotics for micromanipulation*. John Wiley & Sons, 2010.
- [14] M. Savia and H. N. Koivo, "Contact micromanipulation survey of strategies," *Transactions on Mechatronics*, vol. 14, no. 4, pp. 504–514, 2009.
- [15] J. Dejeu, M. Bechelany, P. Rougeot, L. Philippe, and M. Gauthier, "Adhesion control for micro-and nanomanipulation," *ACS nano*, vol. 5, no. 6, pp. 4648–4657, 2011.
- [16] J. Thompson and R. S. Fearing, "Automating microassembly with ortho-tweezers and force sensing," in *IEEE/RSJ International Conference on Intelligent Robots and Systems*, vol. 3. IEEE, 2001, pp. 1327–1334.
- [17] A. Bicchi, "On the closure properties of robotic grasping," *The International Journal of Robotics Research*, vol. 14, no. 4, pp. 319–334, 1995.
- [18] J. Ponce and B. Faverjon, "On computing three-finger force-closure grasps of polygonal objects," *Transactions on Robotics and Automation*, vol. 11, no. 6, pp. 868–881, 1995.
- [19] Y. Wu, D. Sun, and W. Huang, "Force and motion analysis for automated cell transportation with optical tweezers," in *9th World Congress on Intelligent Control and Automation (WCICA)*. IEEE, 2011, pp. 839–843.
- [20] D. J. Cappelleri, M. Fatovic, and U. Shah, "Caging micromanipulation for automated microassembly," in *International Conference on Robotics and Automation (ICRA)*. IEEE, 2011, pp. 3145–3150.